Student thesis series INES nr 544

Legacy effects of spring temperature anomalies on seasonal productivities in northern ecosystems

Hanna Marsh

2021
Department of
Physical Geography and Ecosystem Science
Lund University
Sölvegatan 12
S-223 62 Lund
Sweden

Hanna Marsh (2021).

Legacy effects of spring temperature anomalies on seasonal productivities in northern ecosystems

Förskjutningseffekter från vårliga temperaturanomalier på säsongsproduktivitet i nordliga ekosystem

Master degree thesis, 30 credits in *Physical Geography*
Department of Physical Geography and Ecosystem Science, Lund University

Level: Master of Science (MSc)

Course duration: *January* 2021 until *June* 2021

Legacy effects of spring temperature anomalies on seasonal productivities in northern ecosystems

---

Hanna Marsh

Master thesis, 30 credits, in *Physical Geography and Ecosystem Science*

Supervisor: Wenxin Zhang, Lund University

Exam committee:
Karin Hall, Lund University
Xueying Li, Lund University

Abstract

Direct and lagged effects from spring temperature anomalies for the time-period 2001-2018 have been investigated for northern ecosystems ($> 30°$N). Three different data sets of Gross Primary Production (GPP) estimates (GOSIF, NIRvGPP and FLUX GPP) have been used in tandem with concurrent climate data to find significant correlations between spring growth and temperature anomalies and subsequent growing seasons.

Estimates show lagged effects from spring temperature (T_{spring}) anomalies are most pronounced in the summer season, and affect the arctic plant production positively; spring warming possibly lessens the harsh climatic constraints that normally govern arctic grasslands and shrub-lands. Below the arctic circle, lagged effects are mainly negative; this strengthens the hypothesis that warm springs and increased vegetation in spring will increase transpiration rates and increase water demands, leading to increased water-stress in summer and autumn. Soil moisture is the dominant control of summer vegetation growth in temperate regions.

However, the signal of climate variables controlling vegetation growth also seems to differ depending on the methods used to estimate GPP, which highlights the importance of higher resolution data-sets to fully understand the underlying mechanisms affecting plant production and plant phenology.

Sammanfattning

Direkta och eftersläpande effekter från ovanligt varma vårar har undersökts för tidsperioden 2001-2018 i norra ekosystem ($> 30°$N). Tre olika dataset för bruttoprimärproduktion (BPP) som betecknar växtlighetens produktivitet, har använts tillsammans med samtida klimatdata för att finna signifikanta korrelationer mellan vårlig BPP, temperaturanomalier och efterföljande säsongers produktivitet.

Eftersläpningseffekter från vårliga temperaturanomalier har kunnat påvisas och är som mest distinkta under sommarsäsongen. Den arktiska och sub-arktiska växtligheten påverkas positivt, troligtvis underlättar ett varmare klimat under våren på de annars mycket hårda förhållanden som råder. Längre söderut är förhållandet det motsatta, vilket stärker hypotesen att varma vårar ökar växtlighetens transpirationsgrad. Därmed ökar växternas behov av vatten, vilket kan leda till ökad torka under sommaren och hösten. Jordfuktighet visade sig även vara en av de viktigaste faktorerna som reglerar växtligheten i de södra regionerna.

En viktig aspekt dock, är att resultaten gällande de klimatvariabler som primärt kontrollerar växtlighet skiljer sig något, beroende på hur BPP har uppmätts och modellerats. Detta understryker betydelsen av att fortsätta utveckla nya och bättra dataset, med högre upplösning, för att vidare förstå de underliggande mekanismerna som omgärdar växtproduktivitet och dess fenologi.

Contents

1 Introduction

The last decades have seen an increase in global temperatures, leading to changes to the timing of thermal growing seasons and phenological cycles of plants. Earlier onsets of spring, increased frequency of droughts as well as changing precipitation patterns have been observed (IPCC, 2014). These changes are thought to induce direct and lagged effects on gross primary production (GPP), the gross uptake of carbon dioxide (CO_2) by plant photosynthesis, as well as various climate feedbacks.

The direct impact on GPP from seasonal warming, drought, and drought-related variables (e.g., soil moisture, atmospheric vapor pressure deficit, heat stress and forest fires) is well studied in northern ecosystems: spring warming directly affects the onset of leaf growth, leading to increases in spring GPP, meaning there is a general greening of the vegetation (Piao et al., 2015); summer warming mainly has a greening/net positive effect in stimulating GPP across many ecosystems, except for cool and dry Arctic tundra sites, where a browning/dampening effect on vegetation productivity is a prevalent response (Berner et al., 2020); autumn warming has delayed the senescence of plants and enhance both photosynthesis and soil mineralization and litter decomposition rates, however, higher respiration, offsetting increased GPP, leads to a net CO_2 loss in northern ecosystems (Piao et al., 2008). Data from summer droughts- or heatwaves of the last two decades suggest that these events massively affect the productivity of crop- and forestlands and increases water use efficiency; these browning trends are a general cause of concern as it affects food stability, as well as reducing the ability of the vegetation to act as a carbon sink (Peters et al., 2018; Smith et al., 2020).

The lagged responses of ecosystem seasonal GPP to spring temperature anomalies are less known and many climate models struggle to implement them. As noted by Buermann et al. (2018), most carbon-cycle models seem to overestimate the positive lagged effects on GPP caused by spring warming and underestimate the potential influence of built-up water stress and fixed leaf lifespans. To accurately assess direct and lagged warming impacts on terrestrial vegetation is important, as vegetation is a key component of the global carbon, water and energy cycles and tied to biogeochemical and biophysical climate feedbacks. A proper understanding of these highly dynamic systems is crucial, particularly for our general ability to accurately predict and mitigate climate impacts, as well as adapting our societies to a changing climate (Zhang et al., 2017).

Recent work by Buermann et al. (2018) and Bastos et al. (2020) seem to indicate that annual GPP can be both suppressed or stimulated by spring cooling/warming and the consequence depends on a combination of several factors, including climate and environmental conditions, vegetation composition and phenological responses of vegetation but as of now a comprehensive understanding of how these factors interplay remains lacking. The geographical pattern, timing and magnitude of such lagged responses are also uncertain (Xia et al., 2014; Buermann et al., 2018; Bastos et al., 2020).

The analysis was based on high-resolution climate and GPP datasets (2000-2018), at a spatial resolution of 0.05° ($\sim$ 5x5 km^2, versus 50x50 km^2 in Buermann et al. (2018) and Bastos et al. (2020)). Such high resolution can explicitly explore spatial details and

differences in responses of ecosystem production per biome. Further, the main GPP data sets are derived from near-infrared reflectance (NIR) or Solar-Induced chlorophyll fluorescence (SIF), which are regarded as novel GPP proxies, better reflecting photosynthetic activity compared to conventional satellite-derived vegetation indices, like Normalized Difference Vegetation Index (NDVI) or Enhanced Vegetation Index (EVI) (Li and Xiao, 2019).

The main hypothesis can be stated as: lagged responses of spring warming or cooling will stimulate or suppress GPP in the summer, this depends on: amplified or dampened water stress, the sensitivity of plant species to summer warmth and changes in soil conditions. The summer response of GPP can further affect the autumn phenology, that is, advance or delay the senescence of plants. Therefore, the main aims are to answer the following questions:

1. What is the geographical distribution and pattern of lagged responses of spring temperature anomalies?

2. What is the process of transition between positive to negative impacts on GPP and vice versa and how long does it take for lagged effects to set in?

3. What is the aggregated impact (positive, negative, or neutral) for each biome?

4. The climatic drivers behind summer and autumn production anomalies will also be assessed; particularly whether lagged effects from spring temperature anomalies or concurrent climate factors (temperature, soil moisture, VPD) can be mainly attributed to causing productivity anomalies in summer and autumn.

2 Background

2.1 Annual and seasonal warming in the Northern Hemisphere

From 1975 and onward, annual temperatures in the Northern Hemisphere have steadily risen with $\sim 0.2°C$ decade^{-1} (Jones and Moberg, 2003; Hansen et al., 2006). The change is most noticeable over landmasses and high latitudes, thus mostly affecting the arctic ecosystems of Alaska and Siberia; these regions have seen changes of $\geq 0.3°C$ per decade (Jones and Moberg, 2003; Schwartz et al., 2006). Seasonal changes in surface temperature also differ greatly, where the spring and winter seasons dominate the changes seen on the annual scale (Cayan et al., 2001; Schwartz et al., 2006). Spring temperatures seem to be of particular importance to Eurasia, where spring temperatures have increased $\sim 0.6°C$ decade^{-1} between 1990-2008. During the same time-period, North America has seen warmer autumns ($\sim 0.5°C$ decade^{-1}) compared to springs ($\sim 0.2°C$ decade^{-1}), which seems to suggest changes in seasonality are unevenly spread. (Piao et al., 2008).

Spring warming is of particular importance to plant phenology and productivity, many biological processes related to plant development and propagation occur in springtime and changing temperatures affect their rate and timing greatly (Badeck et al., 2004).

For instance, Schwartz et al. (2006) find that important spring indices such as first leaf date, first bloom date and last spring freeze all have been put forward between 1-1.5 days decade^{-1} during the 1955-2002 time period. Similarly, Root et al. (2003) reviewed 61 studies of different spring phenology traits and found a mean change in timing of -5.1 ± 0.1 days decade^{-1}. They also found tree species were less affected (-3.0 ± 0.1) compared to non-tree species, which were much closer to the overall mean.

However, a study by Fu et al. (2015) suggests that this well-known response to warming might not continue into the future. By observing the timing of leaf unfolding, between 1980-2013, for seven different tree-species across Europe, the surprising result was that temperature sensitivity has started to decline over the years. A full explanation of this effect has not yet been provided, however, two hypotheses have been put forward: one pertaining to an evolutionary trait found in some plants that makes them enter a dormant state caused by cool winter-temperatures, often referred to as *vernalization*. After which, the plant is prepared to enter the developmental stages seen in spring. This mechanism is thought to offer some protection to frost-damage. However, if wintertime is shortened and less cold, the chilling requirements might not be properly met, causing a delay to plant development and consequently reducing the plant sensitivity to spring warming. (Yu et al., 2010; Fu et al., 2015). The second hypothesis attributes photoperiod (day-length) becoming the new limiting factor, when warming has reached a certain level; this is thought to be particularly true for beech (*Fagus Sylvatica*) forests, which are known for their dependence on day-length (Keenan, 2015; Zohner and Renner, 2015).

Temperature variability is also an important influence on plants. It is projected to increase in the future, which mainly poses a risk to more frequent and damaging frost events in late spring. Consequently, early springs may therefore increase the risk of frost damage, as unfolded leaves lack protection to freezing temperatures, particularly in temperate regions. (Rigby and Porporato, 2008; Augspurger, 2013) However, a lowered temperature sensitivity in spring may counteract this concern. Consequently warming impacts on the seasonal and interannual vegetation growth and phenology are complex and difficult to quantify (Yu et al., 2010).

Propagating legacy effects from early springs are also pending between positive, neutral or negative impacts on seasonal productivity: An early spring may increase the leaf area index, leading to a higher potential for photosynthetic activity. It may also increase nitrogen-mineralization rates in the soil, leading to positive impacts on overall plant growth in the later seasons. (Jin et al., 2020); however, early greening also increases transpiration from plants. Locally, the effect can be dependent on reduced or increased soil moisture, which results from how altered transpiration affects precipitation patterns. Spring greening may therefore have an affect on the productivity of later seasons and can either exacerbate droughts or mitigate them, causing reductions/increases in the following seasonal GPP. (Piao et al., 2019; Lian et al., 2020). The temporal pattern of lagged effects from spring to subsequent summer and autumn productivity is not very well understood. However, earlier springs have been statistically correlated with an earlier autumn senescence; an earlier spring onset of 1 day was linked to an advanced autumn senescence onset of 0.6-days (Keenan and Richardson, 2015).

Another aspect of drought is Vapor Pressure Deficit (VPD). VPD is essentially the difference between the pressure of saturated air and the actual pressure at any given temperature. VPD is strongly correlated with air-temperature, since higher temperatures will increase the vapor pressure at saturation with ~ 7 %/K; increasing VPD is therefore thought to impact the stomatal conductance negatively, leading to lower photosynthetic rates (Yuan et al., 2019).

2.2 Satellite derived indices used as proxy for GPP

Global assessment of GPP is surrounded by much uncertainty but is integral for our understanding of carbon climate feedbacks and ecosystem carbon balance. Many remote sensing methods depend on reflectance data that assesses the structural presence of leaves (Leaf Area Index, LAI) or other types of vegetation indices such as Normalized Difference Vegetation Index (NDVI), Enhanced Vegetation Index (EVI) or the fraction absorbed photosynthetically active radiation by vegetation (fPAR) (Li et al., 2018). One of the most well-used methods is the Light Use Efficiency (LUE) model, developed by Monteith (1972, 1977), that directly relates absorbed PAR and LUE to GPP.

A drawback to these types of methods is that the rapid variability of the photosynthetic reaction does not translate to plant's outward appearance, there is often a significant delay before drought and other types of plant stress have a significant impact on the reflectance value of the plant (Meroni et al., 2009).

Using Solar-Induced Chlorophyll fluorescence (SIF) as a proxy for plant productivity is considered a relatively new method, but has become widely used as of late. The first global estimates were performed using the Japanese Greenhouse Gases Observing Satellite (GOSAT), launched in 2009 (Frankenberg et al., 2014). New launches since then, e.g. the Orbiting-Carbon Observatory-2 (OCO-2) has improved spatial resolution and data quality considerably (Sun et al., 2018).

SIF is essentially light emitted by the plant itself: as sunlight is absorbed by the chlorophyll pigment, a small flux of photons is emitted in response, ranging in wavelength between 600-800 nm (Meroni et al., 2009; Li et al., 2018). The emitted light can be detected from space by measuring the fractional depth of narrow solar absorption bands, often referred to as Fraunhofer bands, as the fluorescence adds a small offset, that can be detected even during moderately cloudy conditions (Frankenberg et al., 2011, 2012). SIF derived GPP has the advantage of more easily capturing rapid changes in productivity, as the emitted SIF directly correspond the functional status of the plant.

However, some uncertainties related to deriving GPP from SIF still remain. SIF has a linear relationship to GPP, but the conversion rate has shown to differ depending on biome-type, which adds some complexity to the process (Li and Xiao, 2019).

Another recently proposed proxy, suggested by Badgley et al. (2017) is called the Near-Infrared Reflectance of vegetation (NIRv). It is the product between the well-known NDVI and the total value of NIR reflectance. NIRv was mainly proposed to help solve two common issues with remotely sensed GPP, one related to mixed signals in pixels where vegetation and non-vegetation is intermingled, the second is the difficulty

in estimating the photosynthetic potential of the vegetation cover. NIRv is essentially the proportion of reflectance in each pixel, that can be attributed to vegetation, thus removing most of the influence from non-vegetation. Secondly Badgley et al. (2017) also noticed NIRv correlates with canopy light-use efficiencies, they believe NIRv has the capacity to capture differences in canopy architecture, which makes it a proxy for photosynthetic potential. In comparison to SIF-derived GPP, NIRvGPP has the advantage of being easily computed, in addition, satellites with technology to measure NIR has existed since 1981, providing a longer time-series.

Remote sensing has been an invaluable tool to scale up plant productivity measurements on a global scale. However, flux towers using the eddy covariance technique to separate carbon fluxes, rather effectively estimates productivity rates locally. It is still the most reliable method on an ecosystem scale. Further, flux towers spread out over the globe has provided a framework for upscaling measurements globally, the most common practice is either machine learning or LUE-models (Joiner et al., 2018).

2.3 Outlook on anomaly years

The Northern Hemisphere has been affected by a number of heat- and drought-waves (HDWs) the past 20 years, contributing to widespread wildfires, crop-failure, human casualties and reduced ecosystem carbon uptake (Li et al., 2021). Some notable HDWs include: Western/Central Europe in 2003 (Reichstein et al., 2007), Eastern Europe and Western Russia in 2010 (Barriopedro et al., 2011), North America in 2011-2012 (Sun et al., 2015), Southern China in 2013 (Yuan et al., 2016) and lastly Northern/Central Europe in 2018 (Barriopedro et al., 2020). Some of the events were extreme on an unprecedented scale: the European heatwaves of 2003 and 2010 broke a 500 year long summer-seasonal heat record in many regions. The record lasted until 2018, when it was broken yet again. (Barriopedro et al., 2011; Bastos et al., 2020).

These HDWs are expected to occur more frequently as a side-effect of global warming; Christidis et al. (2015) conclude that previous twice in a century events now are projected to occur twice a decade instead. The heat-waves of the past 20 years can thus, in many ways, be considered proxies of a new climate normal.

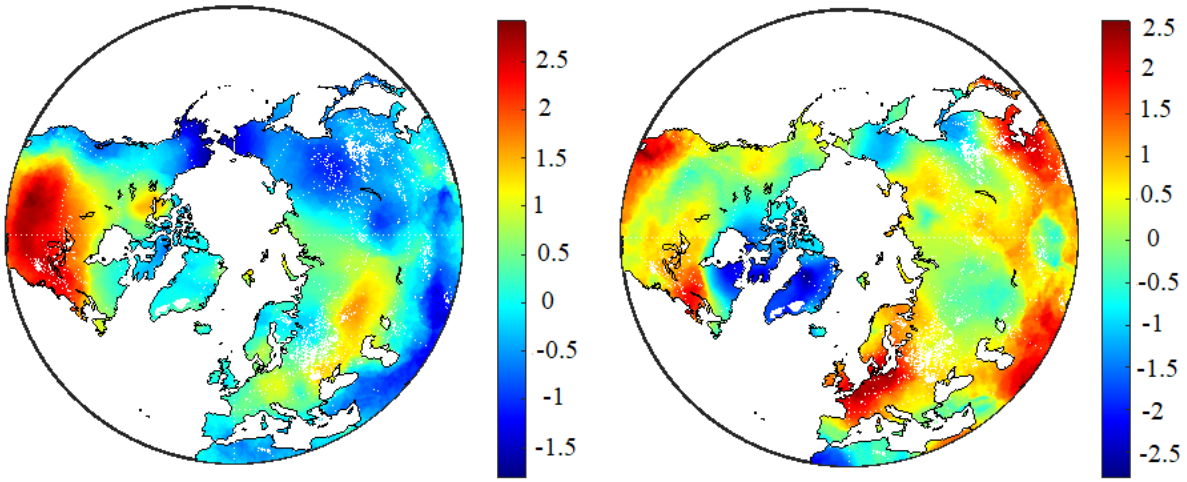

(a) Spring 2012 (b) Summer 2018

Figure 1: Temperature anomalies presented as standard deviations σ for the study period 2001-2018 (a) The Spring season of 2012 was exceptionally warm in North America (b) The Summer of 2018 was exceptionally hot and dry for northern and central Europe.

3 Methodology

3.1 Study area

The study area covers vegetated areas north of 30° in the Northern Hemisphere, an estimated land area of $\sim$ 41 million square kilometres encompassing several different vegetated land cover types: from the Arctic/subarctic tundra in the north to temperate forests and grasslands in the south. Regions located above 30° are characterized by having a strong annual growing seasonality: spring (March, April, May), summer (June, July, August) and autumn (September, October, November), which is not the case further south, where other types of seasonality patterns dominate. A map representation of the study area is seen in Figure 2.

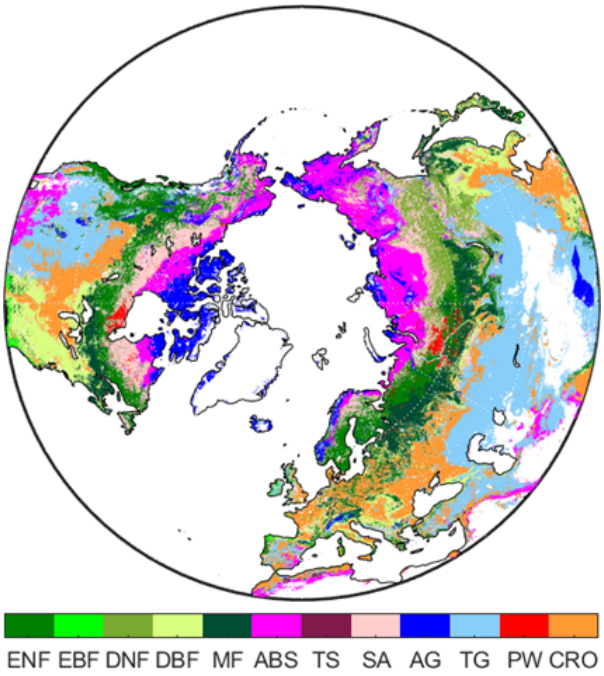

Figure 2: In total, 12 biomes in the study area comprise Evergreen Needleleaf Forests (ENF), Evergreen Broadleaf Forests (EBF), Deciduous Needleleaf Forests (DBF), Mixed forests (MF), Arctic and Boreal Shrublands (ABS), Temperate Shrublands (TS), Savannas (SV), Arctic Grasslands (AG), Temperate Grassland (TG), Permanent wetlands (PW), and Croplands (CRO).

The land-cover classification used in this study was based on the global 0.05° land cover type datasets of 2011 (Friedl and Sulla-Menashe, 2015) and the Köppen–Geiger climate map (0.01° in the spatial resolution) of the world (Kottek et al., 2006; Peel et al., 2007). Friedl and Sulla-Menashe (2015) used the biome classification scheme of the International Geosphere-Biosphere Programme (IGBP), which mainly bases land cover type classification by NDVI thresholds. Grasslands were divided into temperate and arctic grasslands, to separate alpine and high arctic tundra from low-laying temperate grasslands; further, shrublands were divided into temperate and arctic and boreal shrublands. Approximately 19% of the study area is temperate grasslands, making it the most extensive biome, followed by arctic boreal shrublands (15%). In contrast the smallest biomes are temperate shrublands (0.13%) and evergreen broadleaf forests (0.34%), a more thorough description of each biome-type is given in Table 1.

Table 1: Definitions of the 12 biome-types, developed by Sulla-Menashe and Friedl (2018). Grass- and shrublands were further divided according to (Kottek et al., 2006).

Name	Short name	Description
Evergreen Needleleaf Forest	ENF	Dominated by Evergreen Conifer trees, (canopy>2m). Tree cover >60%
Evergreen Broadleaf Forest	EBF	Dominated by evergreen broadleaf and palmate trees (canopy>2m). Tree cover>60%
Deciduous Needleleaf Forest	DNF	Dominated by deciduous needleleaf (larch) trees (canopy>2m). Tree cover>60%
Deciduous Broadleaf Forest	DBF	Dominated by deciduous broadleaf trees (canopy>2m). Tree cover>60%
Mixed forests	MF	Mix between deciduous and evergreen (40-60% of each tree type) (canopy>2m). Tree cover>60%
Arctic Boreal shrublands	ABS	Dominated by woody perennials (1-2m height)
Temperate Shrublands	TS	Dominated by woody perennials (1-2m height)
Savannas	SA	Tree cover 10-30% (canopy >2m).
Arctic Grasslands	AG	Dominated by herbaceous annuals (<2m).
Temperate Grasslands	TG	Dominated by herbaceous annuals (<2m).
Permanent Wetlands	PW	Permanently inundated lands with 30-60% water cover and >10% vegetated cover.
Croplands	CRO	At least 60% of area is cultivated cropland.

3.2 Data-sets

Three different data-sets of GPP have been used in this project.

The GOSIF GPP data-set, provided by Li and Xiao (2019) can be retrieved freely from (`https://globalecology.unh.edu/`). It is based on measurements made by NASA's sun-synchronous and polar orbiting Carbon Observatory-2 (OCO-2) (launched 2014). SIF retrieved by OCO-2 has a higher resolution (1.3x2.25 km^2) and data acquisition rate compared to e.g. GOSAT or Global Ozone Monitoring Experiment (GOME). Still, measurements are too temporally and spatially sparse to provide a data-set with 0.05° and 8-day time-step resolution (converted into monthly for this project). Li and Xiao (2019) have used eight biome-specific linear relationships between SIF and GPP, in combination with machine-learning techniques to create a global coverage (0.05°) of SIF-based GPP from the year 2000-present. Climate data, such as air temperature, photosynthetic active radiation (PAR) and VPD was used in combination with the Enhanced Vegetation Index (EVI) retrieved by the Moderate Resolution Imaging Spectrometer (MODIS) to help with calibration of SIF. Li and Xiao (2019) compared GOSIF to GPP retrieved by 91 Eddy-Covariance (EC) FLUXNET measurement towers to estimate GPP, and found a strong correlative relationship between the two (R^2=0.71, $p < 0.001$).

Table 2: Main data-sets used in the project. Bilinear interpolation was used to convert the ERA5land climate data from 0.1° to 0.05°.

Name	Resolution	Time span	Type
GOSIF GPP	0.05°, monthly	2001-2018	TIF
NIRvGPP	0.05°, monthly	2001-2018	netcdf
FLUX GPP	0.05°, monthly	2001-2018	nedcdf
Landcover MCD12C1 v006	0.05°, yearly	2011	-
ERA5land (air temp, soil moisture and VPD)	0.1°, monthly	2001-2018	netcdf

The global NIRvGPP data-set is based on measurements made by the Advanced Very High Resolution Radiometer (AVHRR) and provided by Wang et al. (2021). Similarly to GOSIF GPP, they used measurements from EC flux-towers to calibrate and validate empirical relationships between NIR-GPP. 104 towers were utilized in total. The flux-towers were separated based on 10 different biomes. The resulting model was upscaled to create a global coverage. Their model yielded a mean of $R^2 = 0.70$ for the validation sites. The NIRvGPP data-set uses no climate data as input.

The third data-set of global GPP is provided by Joiner et al. (2018). They used a simplified LUE-based model framework, with no other meteorological inputs. LUE was retrieved from the MODerate-resolutionImaging Spectroradiometer (MODIS). Concurrently, they used both SIF and NIRv as GPP proxies, mainly to highlight regions of high productivity. Their set of modelled GPP was then calibrated against the FLUXNET 2015 GPP dataset.

3.3 Pretreatment of the data

The spatial resolution of all data-sets in this project needs to be aligned and compatible to be able to produce viable correlations. The spatial scale chosen for this project is 0.05°, and data with a lower resolution thus needs to be converted. This conversion was performed using 2-dimensional linear interpolation. The spatial resolution (0.05°), that each pixel covers varies across the study-area, and mainly depends on the latitude; hence, further north the pixels cover a smaller area than in the south, however, this is believed to have a marginal effect on the results, since the GPP-products are measured as densities (meaning they are area-independent), rather than quantities.

The correlations between climate variables were not performed using measured values but between anomalies. The definition of anomalies were based on z-score statistics according to equation 1.

$$z = \frac{x - \mu}{\sigma} \tag{1}$$

Where μ is the seasonal mean of the whole time-period per grid-cell and σ the standard deviation. The raw number x can thus be more easily interpreted in terms of standard deviations and whether the anomaly is positive or negative compared to the seasonal mean.

Lastly subsets of data was created by choosing pixels based on two requirements. The environmental controls on browning was of particular interest, so pixels with $< -1\sigma$ for summer/autumn GPP was picked, with the added condition of there being a significant ($p < 0.05$) negative correlation between spring temperature and summer/autumn GPP. These subsets were time-independent, meaning years were intermingled. Consequently maps could not be created from these sub-sets.

3.4 Pearson correlations between T_{spring} anomalies to summer and autumn GPP

The main approach for assessing legacy affects on plant productivity have been to create maps of statistically significant Pearson's partial correlations. Mainly two sets of correlation variables have been used, one pertaining summer GPP and the other for autumn GPP anomalies, see Table 3, direct correlations between spring temperature and spring GPP anomalies were also performed, to get a broader view of the transition trends. Possible covarying effects between climate variables are accounted for when performing partial correlations. This yields a more clear picture of the degree of correlation between any individual climate variable and summer/autumn GPP. The correlations were based on 18 years of data (2001-2018) per individual grid-cell. The statistical significance was tested based on p-values; only correlations with ($p < 0.05$) were kept. The set of variables were chosen to see how lagged effects from pre-season GPP anomalies correlate to summer/autumn GPP anomalies and how it compares to direct climate effects from soil moisture, air temperature and VPD anomalies. The dominating variable per grid-cell was determined by selecting the maximum value (absolute value) to create a spatial

representation of which out of pre-season GPP, soil moisture, air temperature and VPD that dominates in regulating seasonal plant productivity.

Table 3: A direct correlation between spring T and GPP, as well as two sets of variables (pertaining to summer and autumn GPP anomalies) were used in correlation analysis. All variables were converted into anomalies based on equation 1 before Pearson correlations were performed.

X: Predictive climate variables	**Y**
Spring: T	**Spring** GPP
Spring: T, GPP **Summer:** Soil moisture, T, VPD	**Summer** GPP
Spring: T, GPP **Summer:** T, GPP **Autumn:** Soil moisture, T, VPD	**Autumn** GPP

The T_{spring} anomaly correlation to summer and autumn productivity was further investigated by looking at the transition pattern between summer and autumn. Eight transition-patterns were identified: $+-$, $-+$, $++$, $--$, $+/$, $-/$, $/+$ and $/-$. The plus, minus and slash signs denotes positive, negative or insignificant impact respectively, and the position reveals whether it affects summer or autumn GPP. Further, the statistical spread of T_{spring} anomaly correlations were also determined per biome-type, to assess whether the aggregated overall impact could be considered neutral, positive or negative. The mean value of the correlation coefficients grouped per biome-type was determined as the defining factor of this.

3.5 Importance of variables per biome

A slightly different approach was taken when investigating the importance of pre-season GPP, soil moisture, air temperature and VPD to plant productivity in each biome. The data was split into a subset, where the goal was to find pixels that show clear sign of browning. Mainly two conditions were applied: (1) $\leq$ 1sd below the seasonal mean of GPP and (2) The correlation coefficient between T_{spring} and summer/autumn GPP anomalies < 0. The importance calculation was thus only performed based on data with a clear browning signal.

Two regression ensembles using the sets of variables in Table 3 were created using the built-in matlab function Least-Squares boosting (LSBOOST). The function iteratively builds a predicted value $f(x_n)$ of plant productivities and compares it to the observed value y_n for each iteration n. The mean-square error is minimized at every iteration according to the algorithm developed by Friedman (2001).

The importance of each x-variable to the modelled plant productivity was extracted using the built-in function predictorImportance, which sums the change in the risk of node-splitting and divides by the number of decision-tree branches (Mathworks, 2021). The resulting number is a qualitative measure of how important each variable is to the modelled plant productivity. The relative predictor importance numbers were converted

into percentages. For this analysis, only GOSIF and NIRvGPP were used due to time-constraints.

3.6 General overview of methodology

An overview of the work-flow in this project is given in Figure 3, which illustrates the order of the main procedures. All procedures were performed using Mathworks MATLAB, version 2020a.

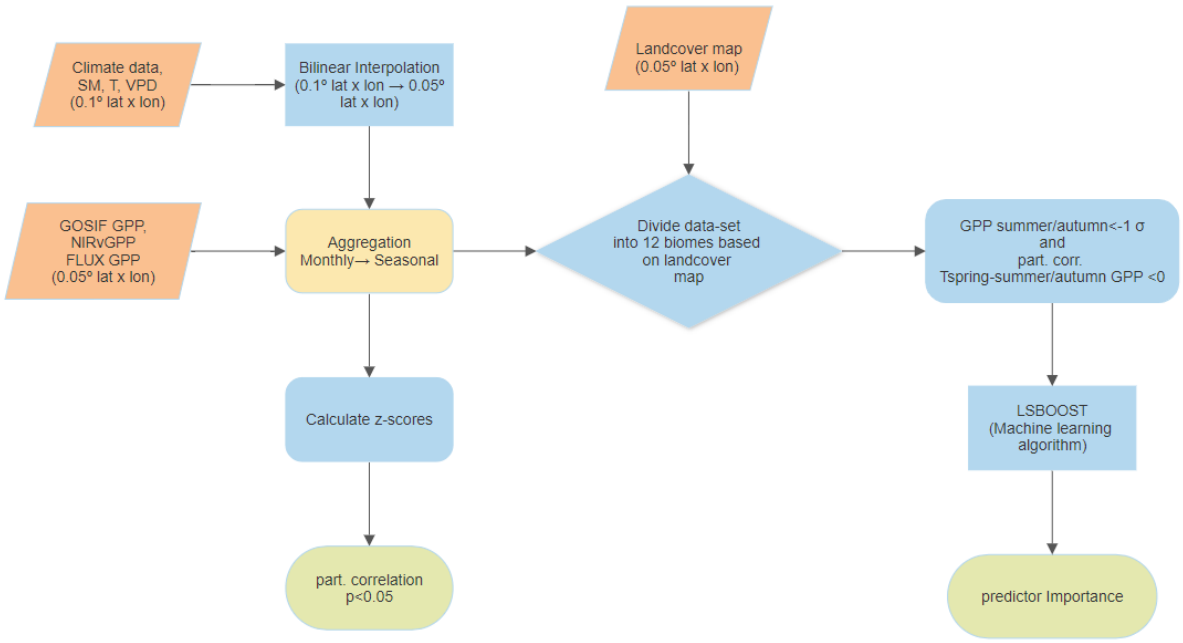

Figure 3: The input data (depicted in red color) underwent several procedures and calculations, eventually leading to the main results (depicted in green).

4 Results

4.1 Years of temperature anomalies between 2001-2018

The number of anomalous warm/cold springs were defined as $T_{spring} > +1\sigma$ or $T_{spring} < -1\sigma$. The spatial distribution, see Figure 4, indicates a patchy behaviour with a range between 1-6/0-6 years of warm/cold springs between 2001 and 2018. The spatial pattern for warm springs is not particularly decisive; possibly hinting towards a small latitude gradient, where 1-2 warm springs more commonly occurred in the south, and 3-4 in the north. The number of cold springs do not have any hint of a similar gradient. Looking at the statistical distribution across biome-types, see Figure 5, a mean of 3 warm/cold springs holds true for all of them. The forest biomes: ENF, EBF, DNF and MF have a much more contained distribution close to 3, whereas the grass- shrub- and wetlands have a somewhat wider distribution. This result is important to contextualize with regards to anomalies being highly dependent on the extent of the considered time-period. The last two decades are often considered to be the hottest since measurements began, meaning some seasons that are not considered anomalous between 2001-2018, most likely would be considered so in the time-period of 1900-2018.

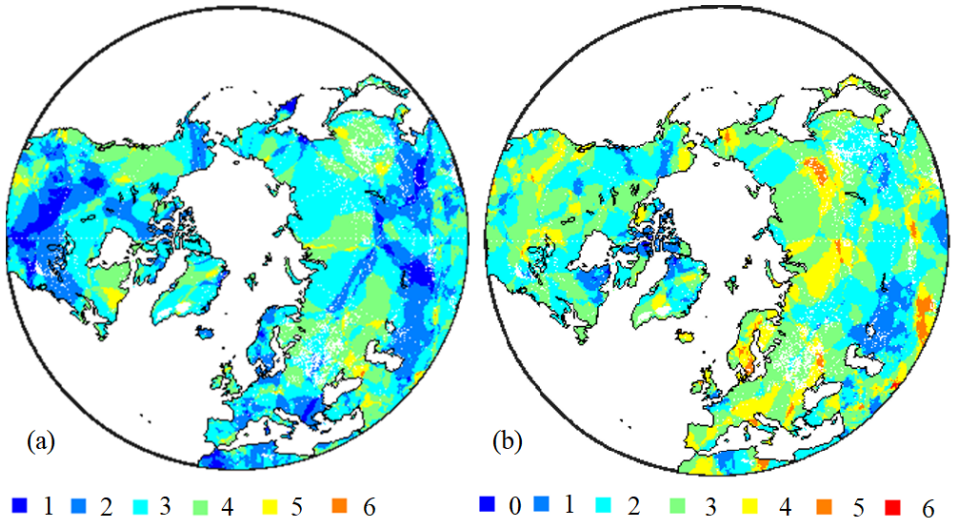

Figure 4: (a) Number of warm springs $> 1\sigma$ (b) Number of cold springs $< 1\sigma$

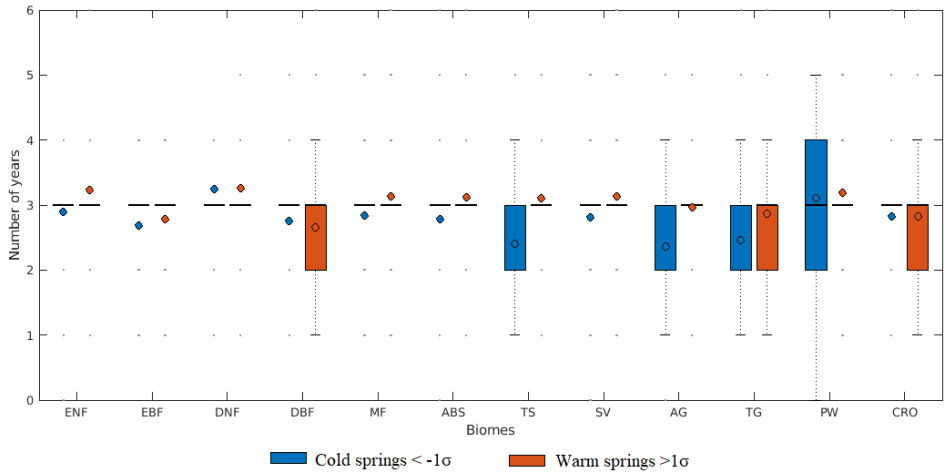

Figure 5: Number of warm/cold springs per biome-type. Line depicts the median and circle the mean value.

4.2 Direct Spring correlations

Direct correlations between Spring temperature anomalies and Spring GPP was performed, see Figure 6. All three products: GOSIF, NIRv and FLUX GPP indicate the same pattern: a strong positive correlation dominates the north and mid-latitudes. Only the southwestern part of North-America and southern Asia see a negative correlation. The same signal is seen for all three products, however, NIRvGPP has fewer significant correlations, resulting in a sparser pattern.

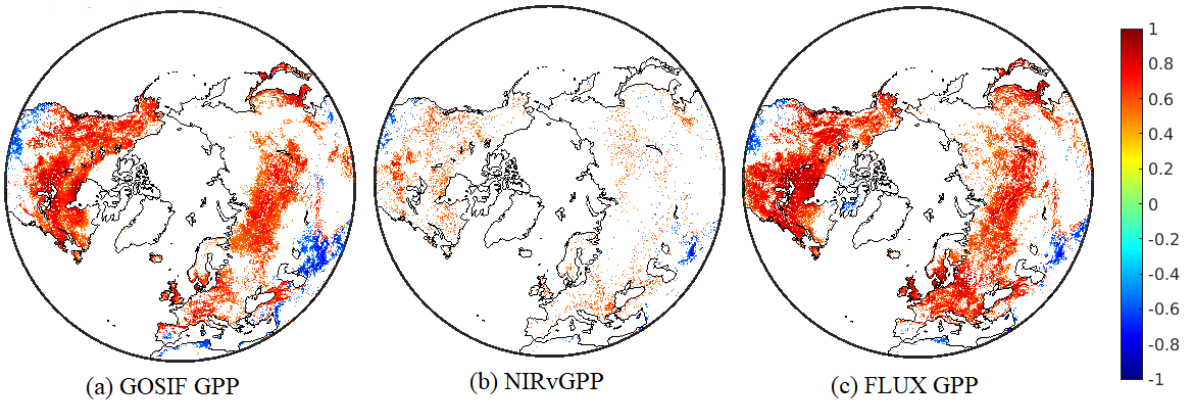

Figure 6: Significant ($p < 0.05$) Pearson's correlations, between Spring temperature anomalies and Spring GPP anomalies.

4.3 Legacy effects from Spring to Summer GPP

Significant partial correlations ($p < 0.05$) between Spring and Summer GPP (Figure 7). The signal differs greatly between the three products, GOSIF has a north-south gradient, with negative impacts dominating the north and positive in the south. NIRvGPP overall has negative impacts, whereas FLUX GPP overall has positive impacts.

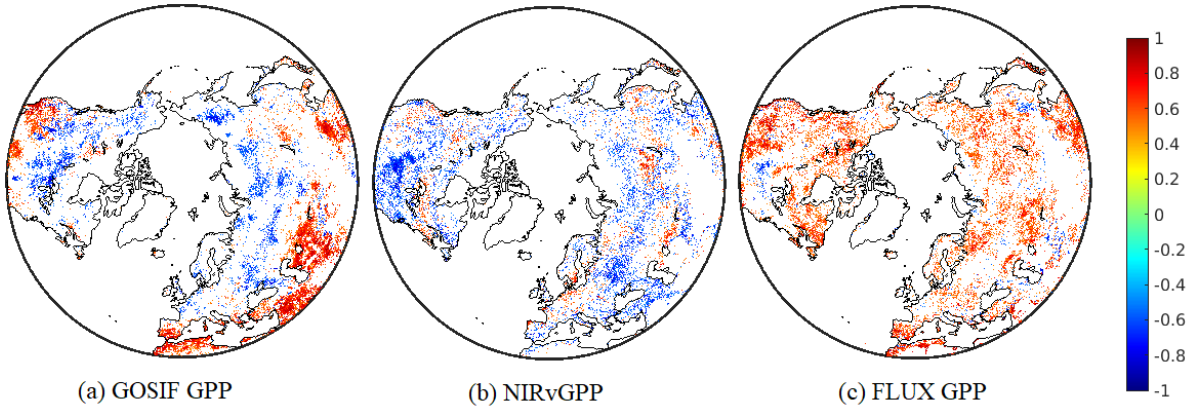

(a) GOSIF GPP (b) NIRvGPP (c) FLUX GPP

Figure 7: Significant ($p < 0.05$) partial Pearson's correlations of Spring to Summer GPP anomalies. The covarying influence from summer VPD, T and soil moisture is accounted for, see Table 3

Lagged effects from T_{spring} anomalies on summer GPP (Figure 8) show fairly similar effects on certain land-areas, but differing on others. In particular negative effects are seen in North America as well as south-east Eurasia. The arctic see clear positive effects for GOSIF and FLUX GPP, whereas negative effects dominate the response for NIRvGPP.

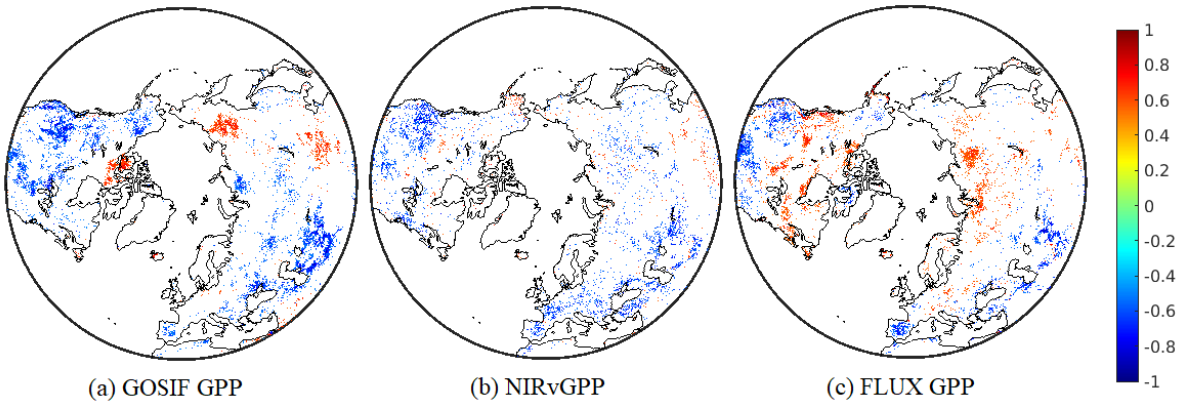

(a) GOSIF GPP (b) NIRvGPP (c) FLUX GPP

Figure 8: Significant ($p < 0.05$) partial Pearson's correlations of T_{spring} to summer GPP anomalies. The covarying influence from summer VPD, T and soil moisture is accounted for, see Table 3.

4.4 Legacy effects from Spring to Autumn GPP

Spring GPP correlations to autumn GPP (Figure 9). Results differ between products, GOSIF GPP sees an overall positive response, particularly in the southern latitudes, whereas NIRvGPP sees more negative impacts. FLUX GPP has a more patchy behaviour with positive and negative impacts intermingled. A strong negative trend is seen for the boreal forests (ENF, DNF, MF) in North America.

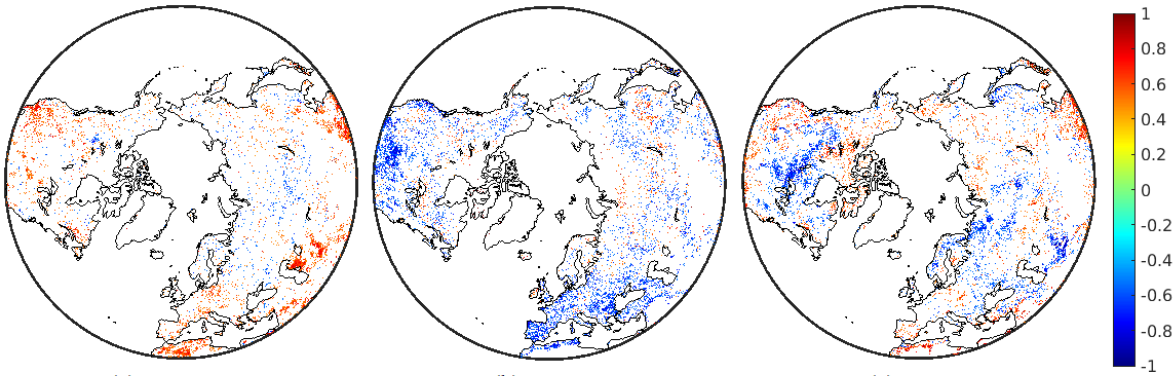

(a) GOSIF GPP (b) NIRvGPP (c) FLUX GPP

Figure 9: Significant ($p < 0.05$) partial Pearson's correlation of spring to autumn GPP anomalies. Covarying climate variables are accounted for, see Table 3.

Legacy effects from T_{spring} anomalies to autumn GPP (Figure 10) are present, but not very consistent between GPP data-sets. GOSIF GPP see a positive influence in North America, but negative for NIRvGPP and FLUX GPP. The general trend is an overall negative impact with some sporadic patches of positive correlations in Eurasia.

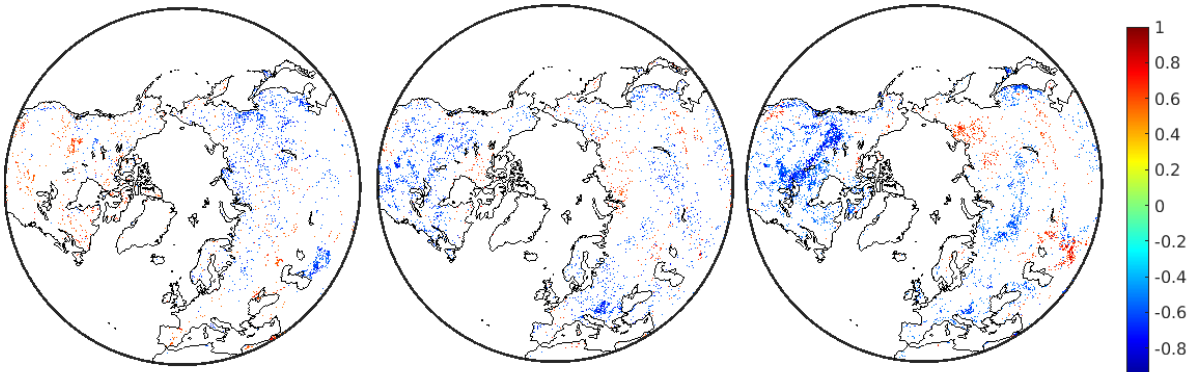

(a) GOSIF GPP (b) NIRvGPP (c) FLUX GPP

Figure 10: Significant ($p < 0.05$) partial Pearson's correlations of T_{spring} and autumn GPP anomalies. Covarying climate variables are accounted for, see Table 3.

4.5 Latitude distribution of Spring Temperature legacy effects

The mean and the range of spring temperature correlation coefficients to summer and autumn GPP are distributed unevenly across latitudes and GPP-products, see Figure 11. GOSIF GPP and NIRvGPP have a fairly similar distribution, even though the autumn signal for GOSIF GPP are closer to zero. FLUX GPP differ from the other two in regards to summer GPP, where positive legacy effects begin to dominate further south, at $\sim 43°$ compared to $> 60°$ for GOSIF and NIRv. FLUX GPP also display a strong negative peak at 55°-60° for autumn GPP, which is almost an inversion of the the legacy effects seen in summer. To summarize, the clearest trend is that areas in southern latitudes are negatively affected by T_{spring} anomalies, switching to positive further up north. The latitude where this switch takes place is not completely analogous for GOSIF, NIRv and FLUX GPP.

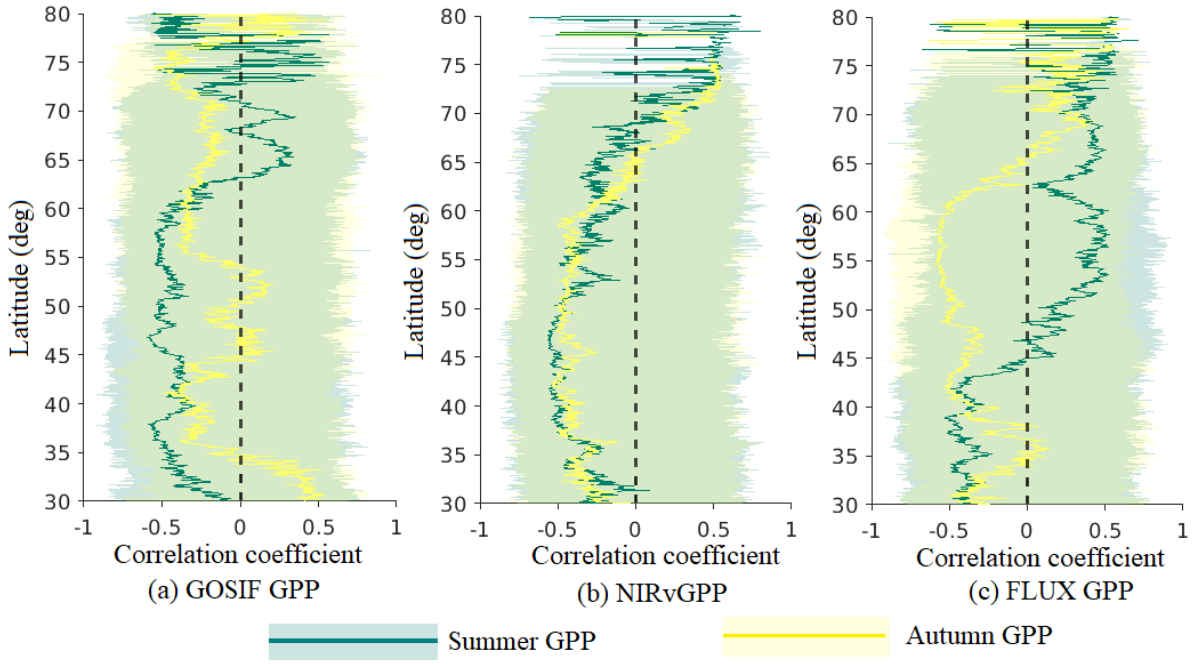

Figure 11: Latitudinal shifts in significant ($p < 0.05$) T_{spring} anomaly correlations to summer/autumn GPP anomalies. The range is depicted as a shaded area and the mean value as a line.

4.6 Dominating correlations

The dominating drivers for summer GPP show a similar pattern for all three products, see Figure 12. The arctic plant productivity is strongly correlated with temperature, whereas temperate regions are dominated by soil moisture. This result works well in accordance with the results seen in Figure 11, even though the direct influence from summer temperature dominates in the arctic. Legacy effects from spring growth also show up as an important factor in a lot of regions, but lagged effects from spring temperature anomalies are not strong enough to surpass the importance of other drivers.

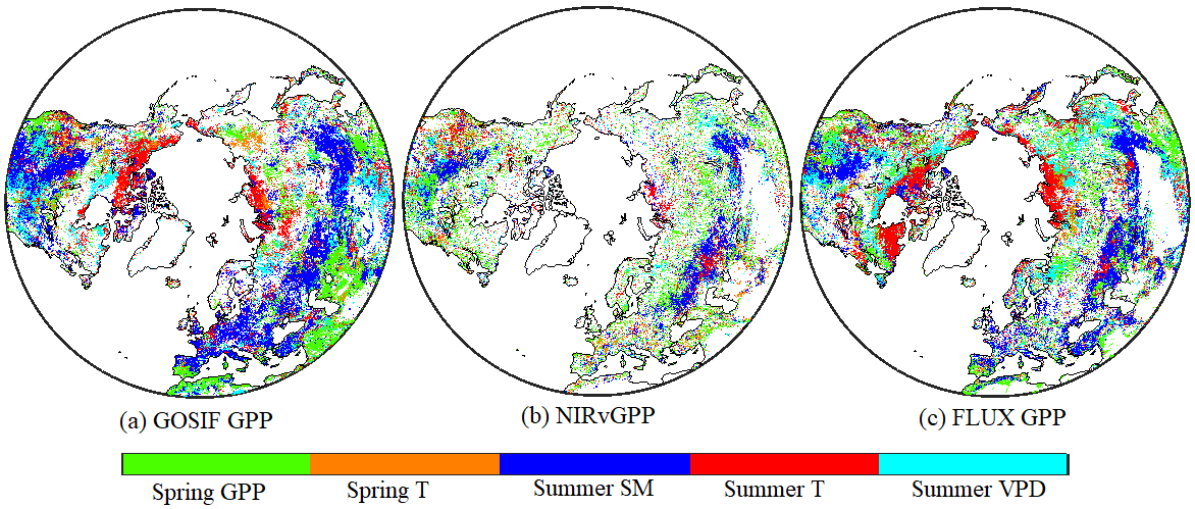

Figure 12: Dominating variable map of correlation anomalies (a) Summer GOSIF GPP (b) Summer NIRvGPP (c) FLUX GPP. The strongest correlation coefficient (absolute value) is depicted. The selection is based on the climate and pre-season sets of variables for summer GPP, see Table 3.

In contrast to summer, the signal for autumn productivity is much more ambiguous, see Figure 13. GOSIF GPP shows a strong dependence on VPD and temperature. For NIRvGPP, the lagged effects from spring productivity show up as important and for FLUX it is the summer productivity in combination with soil moisture that dominate.

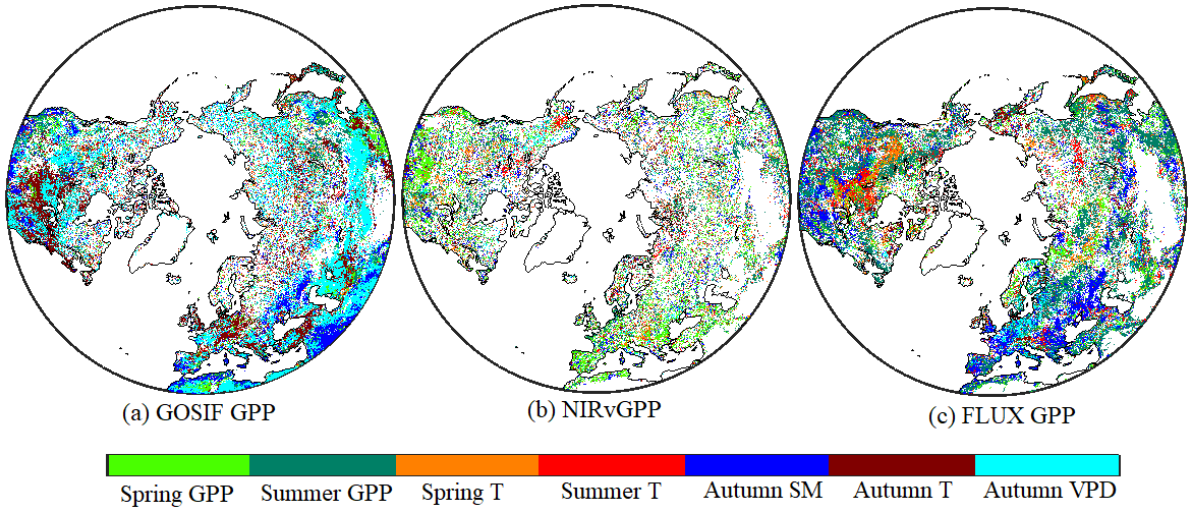

Figure 13: Dominating variable map of correlation anomalies (a) Autumn GOSIF GPP (b) Autumn NIRvGPP (c) FLUX GPP. The strongest correlation coefficient (absolute value) is depicted. The selection is based on the climate and pre-season sets of variables for autumn GPP, see Table 3

4.7 Variables of importance for growth anomalies $< 1\sigma$

The results regarding important drivers for browning in summer and autumn, see Figures 14 and 15 and Table 4. The limiting factor varies depending on biome, but overall for both GOSIF and NIRvGPP datasets, spring GPP shows up as most significant (highest relative importance) for a large portion of them, excluding mainly croplands and boreal shrublands, where soil moisture and temperature dominates.

Table 4: Table of the most significant predictor importance values in % for summer and autumn GOSIF/NIRv GPP. n%-values denote the fraction of available pixels that met the conditions (see methods section for more details) and could be used in the machine-learning algorithm. The R^2-value for each model-ensemble is also given.

	Summer GOSIF GPP				**Summer NIRvGPP**			
Biome	Variable	IMP %	R2	n%	Variable	IMP %	R2	n%
ENF	Spring GPP	86.68%	0.75	29.95%	Spring GPP	35.14%	0.47	13.60%
EBF	Spring T	60.10%	0.82	9.00%	Spring GPP	81.30%	0.89	5.60%
DNF	Spring GPP	68.83%	0.62	8.00%	Spring GPP	33.24%	0.33	18.65%
DBF	Spring GPP	51.90%	0.52	32.43%	Spring GPP	57.67%	0.45	23.44%
MF	Spring GPP	81.86%	0.55	24.98%	Spring GPP	73.02%	0.42	13.10%
ABS	Spring T	65.14%	0.75	14.64%	Summer T	82.64%	0.61	5.62%
TS	Spring GPP	92.06%	0.90	29.36%	Spring GPP	77.16%	0.85	24.61%
SA	Summer VPD	53.86%	0.63	12.45%	Spring GPP	49.94%	0.50	11.54%
AG	Spring T	69.66%	0.75	4.17%	Spring GPP	83.36%	0.80	2.88%
TG	Summer SM	51.00%	0.70	35.38%	Spring GPP	51.15%	0.65	27.45%
PW	Spring GPP	85.96%	0.80	7.94%	Spring GPP	76.90%	0.78	2.87%
CRO	Summer SM	55.99%	0.57	29.06%	Summer T	63.93%	0.66	20.20%
	Autumn GOSIF GPP				**Autumn NIRvGPP**			
Biome	Variable	IMP %	R2	n%	Variable	IMP %	R2	n%
ENF	Spring GPP	76.20%	0.88	7.42%	Spring GPP	88.23%	0.87	12.79%
EBF	Summer GPP	76.19%	0.97	1.36%	Spring GPP	91.72%	0.93	21.65%
DNF	Autumn T	72.42%	0.71	24.84%	Autumn T	58.91%	0.62	5.64%
DBF	Autumn T	76.02%	0.88	11.39%	Spring GPP	81.56%	0.89	27.53%
MF	Autumn T	77.14%	0.88	12.83%	Autumn T	72.46%	0.82	20.94%
ABS	Summer GPP	86.32%	0.82	14.36%	Autumn T	50.99%	0.73	1.32%
TS	Summer GPP	92.13%	0.98	4.00%	Summer GPP	84.48%	0.96	4.07%
SA	Spring GPP	55.91%	0.83	11.42%	Spring GPP	90.20%	0.89	6.97%
AG	Summer GPP	71.68%	0.79	7.20%	Spring GPP	51.21%	0.74	1.12%
TG	Summer GPP	85.52%	0.85	4.61%	Spring GPP	57.97%	0.76	9.95%
PW	Summer GPP	83.10%	0.87	9.13%	Summer GPP	61.14%	0.92	1.91%
CRO	Summer GPP	60.42%	0.77	3.85%	Summer GPP	67.15%	0.65	20.20%

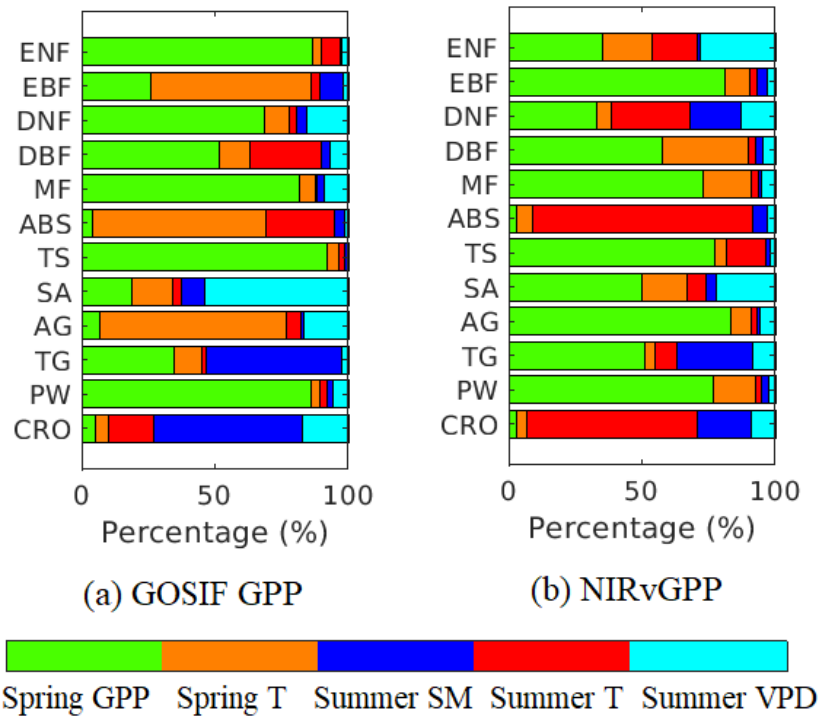

Figure 14: Relative importance (%) of five different climate drivers on summer browning

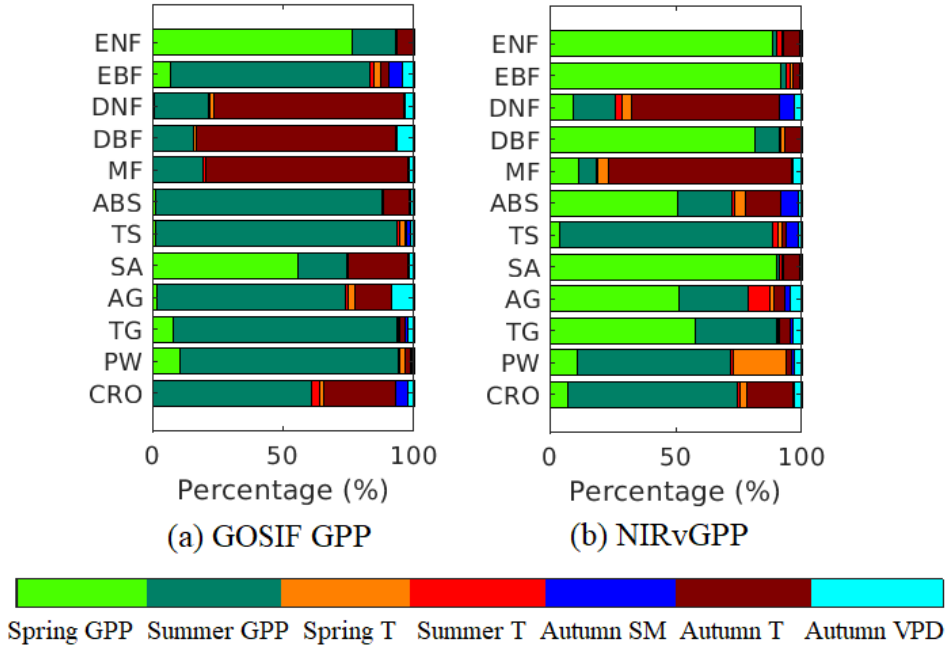

Figure 15: Relative importance (%) of pre-season GPP and temperature as well as autumn soil moisture, temperature and VPD on autumn browning

For GOSIF GPP in particular, the grass- and crop-lands show a very clear dependence on soil moisture, indicating it is the main limiting factor. The fraction of available pixels that met the set conditions of $< -1\sigma$ GPP as well as $p < 0.05$ significant negative correlation between T_{spring} and summer/autumn GPP also varied greatly across biomes, arctic grasslands and wetlands consistently had relatively small fractions of available data-points. R^2 values is a measure of how well the predictor-ensemble can be used to model GPP; overall the majority of $R^2 > 0.5$, and some values indicate a very good fit of $R^2 > 0.8$, particularly so for the TS and EBF biomes.

Further, pre-season plant growth has a high degree of importance for the NIRvGPP and GOSIF GPP data-sets, both for summer and autumn. Temperature is the second most common limiting factor, and mainly controls lowered production rates in autumn for deciduous and mixed forests.

4.8 Transition patterns

How lagged effects from T_{spring} anomalies propagate through the growing season was also a point of interest. The results are presented in Figure 16 and shows maps of the combined effect seen in summer and autumn from T_{spring} anomalies. Insignificant correlations are denoted by / and positive/negative by +/-. The majority of lagged effects set in either in summer or autumn, meaning it is rare to see significant impact during both seasons. GOSIF GPP and NIRvGPP is dominated by a negative impact in summer (-/), whereas FLUX GPP see more of a positive impact in summer (+/) in combination with negative in autumn (/-), meaning the timing of propagating drought differs between GPP data-sets.

Separating the transition patterns based on biomes further reveal the similarity between GOSIF and NIRvGPP, the northern biomes (ABS and AG) show a clear positive impact during summer, whereas FLUX GPP also see positive impact in wetlands (PW), savannas (SV) and DBF during summer.

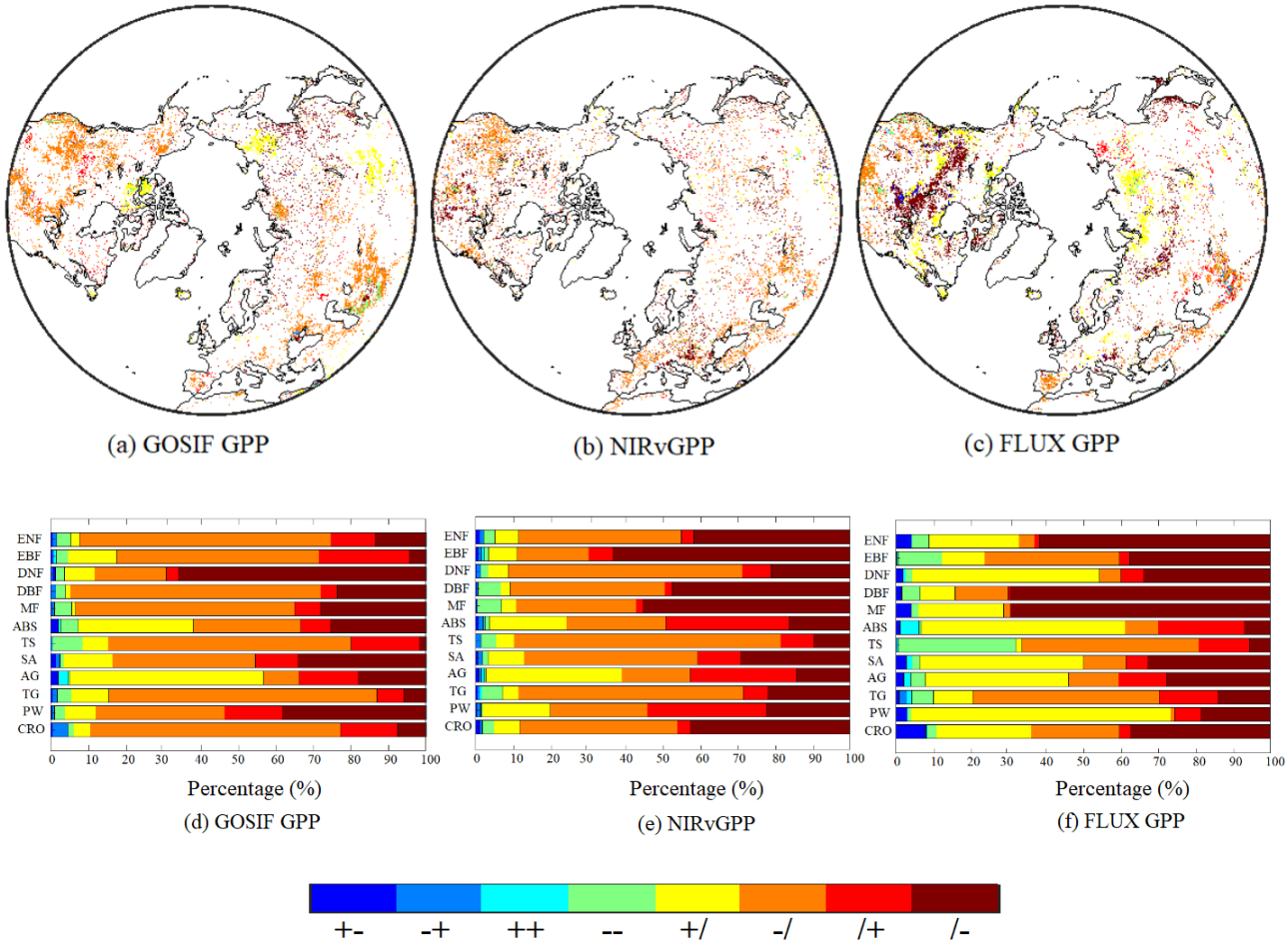

Figure 16: Transition pattern of lagged effects from T_{spring} anomalies on summer and autumn productivity. a)-d) show maps of the combined result from spring temperature anomalies to summer GPP (Figure 8) and autumn GPP (Figure 10. The labels should be interpreted as follows: +- means there was a positive significant impact seen in summer and a negative in autumn, /- means there was an insignificant correlation seen in summer and a significant negative correlation in autumn) e)-f) show relative percentages of a total of 8 different transition patterns (excluding //) per biome-type

4.9 Aggregated impact

Results between GOSIF (Figure 17), NIRv (Figure 18) and FLUX GPP (Figure 19) are similar, but differ on certain points. In general the forest biomes have a smaller statistical spread around negative correlations, meaning the aggregated impact can be said to be negative. The other biomes have a wider statistical spread that stretches across positive and negative impacts, meaning the overall impact is more neutral. FLUX GPP on average, show more positive correlations, particularly in summer, and ABS and AG stand out as the biomes that see an overall positive impact, which implies increased spring temperatures in the far north does not promote drought propagation to the same

extent seen in biomes located further south.

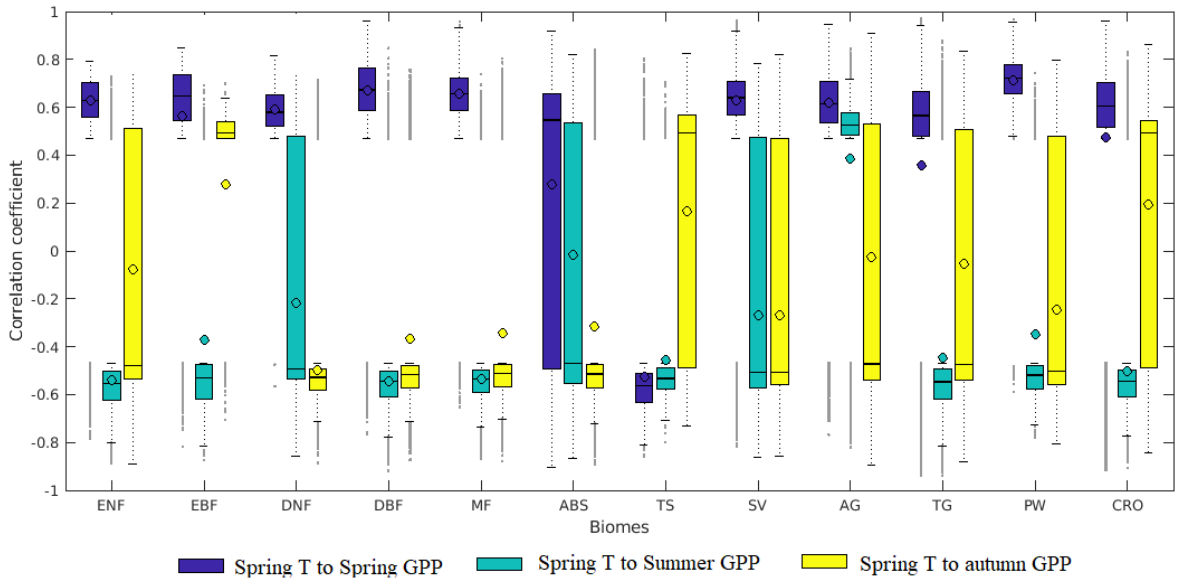

Figure 17: Boxplot of T_{spring} correlation coefficients to seasonal GOSIF GPP. The mean value is represented by a small circle, and median by a line.

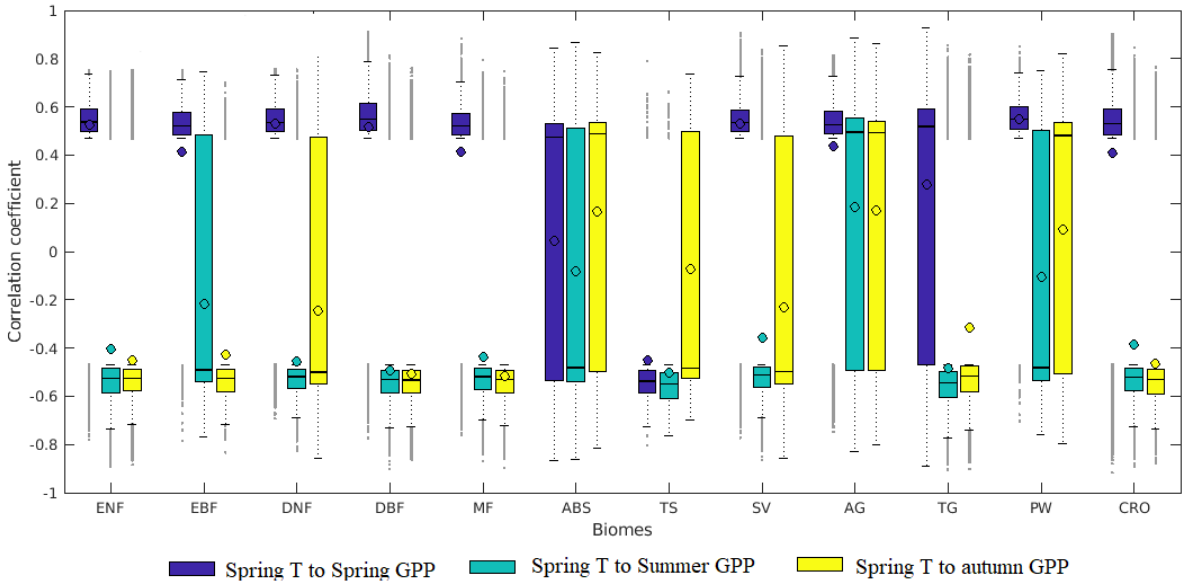

Figure 18: Boxplot of T_{spring} correlation coefficients to seasonal NIRvGPP. The mean value is represented by a small circle, and median by a line.

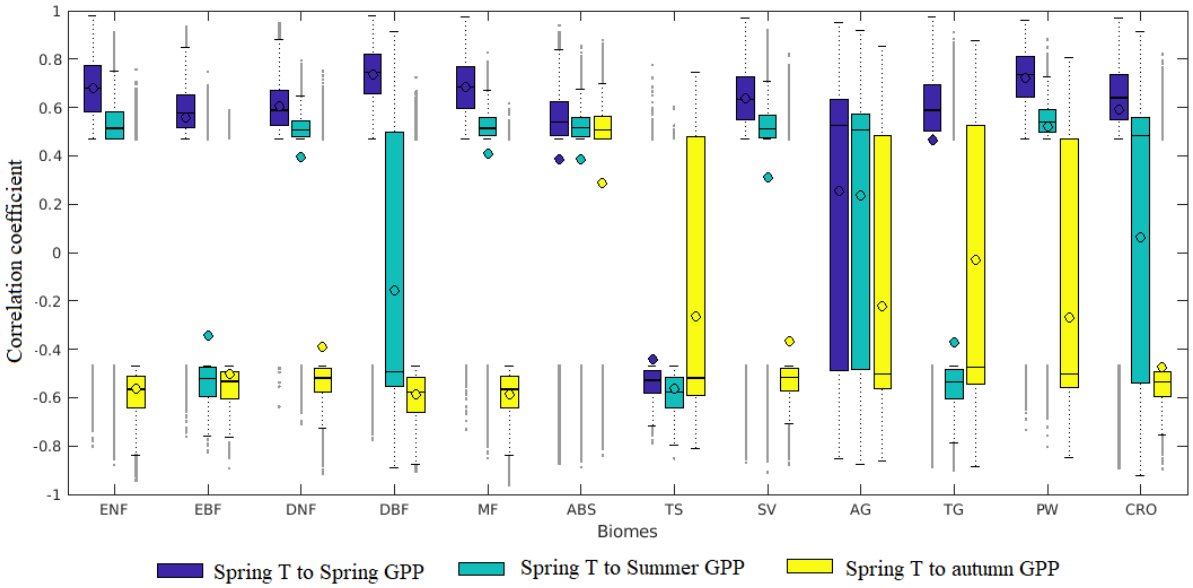

Figure 19: Boxplot of T_{spring} correlation coefficients to seasonal FLUX GPP. The mean value is represented by a small circle, and median by a line.

5 Discussion

The direct impact on spring productivity from T_{spring} anomalies gave a generally coherent result for all three GPP data-sets. For the most part, warm springs and high spring productivities are positively correlated, only the southernmost parts see a negative impact, see Figure 6. The result is relatively reliable, since it holds true for all three products. The results also go hand in hand with Buermann et al. (2018), who found that significant ($p < 0.05$) positive correlations between annual T_{spring} and spring greenness exist and are wide-spread in the Northern Hemisphere.

As discussed earlier in the report, early and warm springs are believed to cause both negative and positive direct impacts on productivity, but these results make a case for the latter being the dominant influence. Damage from e.g. late spring frost-events or acute frost desiccation does not seem to override the growth caused by warming, at least on a global scale.

The strong positive correlation between T_{spring} and spring productivity would lead us to believe that lagged effects from both spring growth and temperature anomalies on subsequent seasons productivity would look fairly similar for all three products. This, however, did not turn out to be the case (compare Figure 7 with Figure 8 and Figure 9 with Figure 10). This result somewhat complicates the relationship between spring productivity and T_{spring} anomalies, as evidently they do not go entirely hand in hand, there are several uncertainties in the data-sets that could contribute to this. One possible explanation, pointed out by Piao et al. (2020), is the difficulty to separate snow-cover decrease from leaf-area increase. The spring months, particularly in the northern-most

regions is often characterized by partial-snow cover. Increasing temperatures might lower the fraction of snow-cover in spring, leading to a false signal of greening.

Significant differences between the GPP data-sets used (GOSIF, NIRv and FLUX) is also a recurring theme in this thesis, which most likely is explained by fundamental differences in the models used to up-scale the data-sets. A notable exception is Figure 12. The results indicate a north-south gradient, where summer temperature is the strongest influence in the northern-most parts. Summer soil moisture together with patches of spring GPP dominate in the mid-latitudes and lagged effects from the growth in spring dominate in the southern parts. The signal is clearest for GOSIF GPP and weakest for NIRvGPP. On average the least amount of significant correlations was seen using the NIRvGPP product, which indicates that NIRvGPP, on average, has a weaker connection to surrounding climate variables than the other two products.

Further, outward disturbances on GPP, such as forest fires, anthropogenic land-cover change or insect-attacks, are not accounted for. Ideally, these factors should be excluded from the analysis due to low significant correlations, but seeing as both GOSIF GPP and FLUX GPP have used machine learning to fill in gaps temporally (GOSIF) and spatially (FLUX), it is likely that these two products are missing the signal from such factors. The modelling used to fill in the gaps for GOSIF and FLUX GPP could also, to some degree, explain the differences seen in dominating drivers between the three products. Climate variables such as soil moisture and temperature were generally considered more important for GOSIF and FLUX, which could be an echo from using climate variables as input to fill in the gaps.

The lagged effects from spring to subsequent seasons were mainly quantified using a partial correlation approach, where the most important drivers related to plant growth were included. Previous research by Zhu et al. (2016) indicate CO_2 fertilization is one of the strongest contributors to the greening trend globally, which in the scope of this project can be viewed as an outside influence, not incorporated in this analysis. However, for the high northern latitudes, temperature increase has been shown to be the main factor facilitating increased plant productivity in summer (Xu et al., 2013; Piao et al., 2020), which is a result that coincides well with Figure 12.

Ideally the results from the three different GPP products used, would have yielded the same signal in terms of which environmental controls that dominate the plant productivity per biome-type. Despite many previous studies reporting strong correlations betweeen NIRvGPP, SIF derived GPP and GPP measured from flux towers, the signal, particularly relating to autumn GPP varied widely (see Figures 13 and 15). One simple explanation of the large differences seen in Figure 13, is that the differences between the strongest correlation coefficients could have been relatively marginal; since only the maximum absolute value was picked, the second and third strongest coefficient could have been what was picked in the other graphs, meaning a cluster of climate variables, instead of a single one control the autumn productivity. This ambiguity is to some degree also reflected in previous research, e.g. Liu et al. (2016) showed that both soil moisture and temperature affect the end of the growing season (EOS), which in this context can be seen as a proxy for autumn productivity; in their study results indicate that the sum

of precipitation during summer delays EOS for grasslands, whereas sum of insolation during summer delays EOS mainly for forest-biomes (ENF excluded).

The transition trends of lagged effects were also of high interest to investigate; results (Figure 16) showed a relatively sparse pattern, where the majority of lagged effects were either -/ or /-. FLUX GPP saw slightly more positive impacts in summer (+/), meaning GOSIF and NIRvGPP coincide to a higher degree. Results also showed that significant impacts generally do not occur in both summer and autumn, indicating the duration-time is limited. Comparing these results to a similar analysis performed by Buermann et al. (2018) on NDVI, the results concur relatively well: the majority of lagged impacts seen were negative (-/ or /-) with some patches of positive (+/) in mainly Eastern and North Eurasia. Buermann et al. (2018) notably points out that this result is not reflected in the majority of carbon-cycle models, which they attribute to them not accurately capturing build-up of water-stress.

The aggregated impact per biome (Figures 17, 18 and 18) were also of great importance to this project. The conclusive signal was that forest biomes clearly showed an aggregation around negative impacts in summer and autumn, compared to the other biomes, where the overall impact could be considered more neutral. A conceivable explanation for the differences seen between forests and shrub-lands is that drought-propagation and other types of plant-stresses caused by warm springs is more pronounced in forests than in shorter vegetation, leading to a stronger overall impact.

6 Conclusions

Propagating impacts from spring growth and temperature anomalies have been shown to affect summer and autumnal productivity in the Northern Hemisphere. These lagged effects are mostly negative and set in either in summer or autumn. The forest biomes (ENF, DBF, MF) show conclusive signals of negative impacts for all three sets of GPP, in summer and autumn, whereas shrub-lands, crop-lands and wetlands have a wider statistical spread between positive and negative impacts, leading to a more neutral overall impact. No biome seem to conclusively have a lagged positive impact from spring temperature anomalies, apart from the northernmost biomes, AG and ABS, which is important to account for in carbon-cycle models. The higher resolution in this project (0.05° compared to e.g. 0.5° of Buermann et al. (2018)) has yielded a more patchy signal of lagged effects, which suggests the spatial pattern of legacy effects show up differently, depending on the scaling of the data-sets used to quantify them.

Results also seem to depend on the type of method used to quantify GPP, which somewhat diminishes credibility. This mainly applies to the main drivers that affect browning and greening trends seen in seasonal GPP; the effect on GPP from increasing temperatures is most likely not linear and many factors are involved. Continuous development of higher resolution GPP data-sets is needed to further assess vegetation response to a warming climate.

References

Augspurger, C. K. (2013), 'Reconstructing patterns of temperature, phenology, and frost damage over 124 years: spring damage risk is increasing', *Ecology* **94**(1), 41–50.

Badeck, F.-W., Bondeau, A., Böttcher, K., Doktor, D., Lucht, W., Schaber, J. and Sitch, S. (2004), 'Responses of spring phenology to climate change', *New phytologist* **162**(2), 295–309.

Badgley, G., Field, C. B. and Berry, J. A. (2017), 'Canopy near-infrared reflectance and terrestrial photosynthesis', *Science advances* **3**(3), e1602244.

Barriopedro, D., Fischer, E. M., Luterbacher, J., Trigo, R. M. and García-Herrera, R. (2011), 'The hot summer of 2010: redrawing the temperature record map of europe', *Science* **332**(6026), 220–224.

Barriopedro, D., Sousa, P., Trigo, R., García Herrera, R. and Ramos, A. (2020), 'The exceptional iberian heatwave of summer 2018', *Bulletin of the American Meteorological Society* **101**(1), S29–S33.

Bastos, A., Ciais, P., Friedlingstein, P., Sitch, S., Pongratz, J., Fan, L., Wigneron, J., Weber, U., Reichstein, M., Fu, Z. et al. (2020), 'Direct and seasonal legacy effects of the 2018 heat wave and drought on european ecosystem productivity', *Science advances* **6**(24), eaba2724.

Berner, L. T., Massey, R., Jantz, P., Forbes, B. C., Macias-Fauria, M., Myers-Smith, I., Kumpula, T., Gauthier, G., Andreu-Hayles, L., Gaglioti, B. V. et al. (2020), 'Summer warming explains widespread but not uniform greening in the arctic tundra biome', *Nature communications* **11**(1), 1–12.

Buermann, W., Forkel, M., O'sullivan, M., Sitch, S., Friedlingstein, P., Haverd, V., Jain, A. K., Kato, E., Kautz, M., Lienert, S. et al. (2018), 'Widespread seasonal compensation effects of spring warming on northern plant productivity', *Nature* **562**(7725), 110–114.

Cayan, D. R., Kammerdiener, S. A., Dettinger, M. D., Caprio, J. M. and Peterson, D. H. (2001), 'Changes in the onset of spring in the western united states', *Bulletin of the American Meteorological Society* **82**(3), 399–416.

Christidis, N., Jones, G. S. and Stott, P. A. (2015), 'Dramatically increasing chance of extremely hot summers since the 2003 european heatwave', *Nature Climate Change* **5**(1), 46–50.

Frankenberg, C., Fisher, J. B., Worden, J., Badgley, G., Saatchi, S. S., Lee, J.-E., Toon, G. C., Butz, A., Jung, M., Kuze, A. et al. (2011), 'New global observations of the terrestrial carbon cycle from gosat: Patterns of plant fluorescence with gross primary productivity', *Geophysical Research Letters* **38**(17).

Frankenberg, C., O'Dell, C., Berry, J., Guanter, L., Joiner, J., Köhler, P., Pollock, R. and Taylor, T. E. (2014), 'Prospects for chlorophyll fluorescence remote sensing from the orbiting carbon observatory-2', *Remote Sensing of Environment* **147**, 1–12.

Frankenberg, C., O'Dell, C., Guanter, L. and McDuffie, J. (2012), 'Remote sensing of near-infrared chlorophyll fluorescence from space in scattering atmospheres: implications for its retrieval and interferences with atmospheric co 2 retrievals', *Atmospheric Measurement Techniques* **5**(8), 2081–2094.

Friedl, M. and Sulla-Menashe, D. (2015), 'Mcd12q1 modis/terra+ aqua land cover type yearly l3 global 500m sin grid v006 [data set]', *NASA EOSDIS Land Processes DAAC* **10**.

Friedman, J. H. (2001), 'Greedy function approximation: a gradient boosting machine', *Annals of statistics* pp. 1189–1232.

Fu, Y. H., Zhao, H., Piao, S., Peaucelle, M., Peng, S., Zhou, G., Ciais, P., Huang, M., Menzel, A., Peñuelas, J. et al. (2015), 'Declining global warming effects on the phenology of spring leaf unfolding', *Nature* **526**(7571), 104–107.

Hansen, J., Sato, M., Ruedy, R., Lo, K., Lea, D. W. and Medina-Elizade, M. (2006), 'Global temperature change', *Proceedings of the National Academy of Sciences* **103**(39), 14288–14293.

IPCC (2014), Climate Change 2014: Synthesis Report. Contribution of Working Groups I, II and III to the Fifth Assessment Report of the Intergovernmental Panel on Climate Change [Core Writing Team, R.K. Pachauri and L.A. Meyer (eds.)], Technical report, IPCC, Geneva, Switzerland, 151 pp.

Jin, J., Guo, F., Sippel, S., Zhu, Q., Wang, W., Gu, B. and Wang, Y. (2020), 'Concurrent and lagged effects of spring greening on seasonal carbon gain and water loss across the northern hemisphere', *International journal of biometeorology* **64**(8), 1343–1354.

Joiner, J., Yoshida, Y., Zhang, Y., Duveiller, G., Jung, M., Lyapustin, A., Wang, Y. and Tucker, C. J. (2018), 'Estimation of terrestrial global gross primary production (gpp) with satellite data-driven models and eddy covariance flux data', *Remote Sensing* **10**(9), 1346.

Jones, P. D. and Moberg, A. (2003), 'Hemispheric and large-scale surface air temperature variations: An extensive revision and an update to 2001', *Journal of climate* **16**(2), 206–223.

Keenan, T. F. (2015), 'Spring greening in a warming world', *Nature* **526**(7571), 48–49.

Keenan, T. F. and Richardson, A. D. (2015), 'The timing of autumn senescence is affected by the timing of spring phenology: implications for predictive models', *Global change biology* **21**(7), 2634–2641.

Kottek, M., Grieser, J., Beck, C., Rudolf, B. and Rubel, F. (2006), 'World map of the köppen-geiger climate classification updated'.

Li, J., Tam, C.-Y., Tai, A. P. and Lau, N.-C. (2021), 'Vegetation-heatwave correlations and contrasting energy exchange responses of different vegetation types to summer heatwaves in the northern hemisphere during the 1982–2011 period', *Agricultural and Forest Meteorology* **296**, 108208.

Li, X. and Xiao, J. (2019), 'Mapping photosynthesis solely from solar-induced chlorophyll fluorescence: A global, fine-resolution dataset of gross primary production derived from oco-2', *Remote Sensing* **11**(21), 2563.

Li, X., Xiao, J. and He, B. (2018), 'Chlorophyll fluorescence observed by oco-2 is strongly related to gross primary productivity estimated from flux towers in temperate forests', *Remote Sensing of Environment* **204**, 659–671.

Lian, X., Piao, S., Li, L. Z., Li, Y., Huntingford, C., Ciais, P., Cescatti, A., Janssens, I. A., Peñuelas, J., Buermann, W. et al. (2020), 'Summer soil drying exacerbated by earlier spring greening of northern vegetation', *Science advances* **6**(1), eaax0255.

Liu, Q., Fu, Y. H., Zeng, Z., Huang, M., Li, X. and Piao, S. (2016), 'Temperature, precipitation, and insolation effects on autumn vegetation phenology in temperate china', *Global change biology* **22**(2), 644–655.

Mathworks (2021), 'Estimates of predictor importance for regression ensemble'. `https://se.mathworks.com/help/stats/compactregressionensemble.predictorimportance.html#bst1m5t-6` [Retrieved 25 April 2021].

Meroni, M., Rossini, M., Guanter, L., Alonso, L., Rascher, U., Colombo, R. and Moreno, J. (2009), 'Remote sensing of solar-induced chlorophyll fluorescence: Review of methods and applications', *Remote Sensing of Environment* **113**(10), 2037–2051.

Monteith, J. (1972), 'Solar radiation and productivity in tropical ecosystems', *Journal of applied ecology* **9**(3), 747–766.

Monteith, J. L. (1977), 'Climate and the efficiency of crop production in britain', *Philosophical Transactions of the Royal Society of London. B, Biological Sciences* **281**(980), 277–294.

Peel, M. C., Finlayson, B. L. and McMahon, T. A. (2007), 'Updated world map of the köppen-geiger climate classification', *Hydrology and earth system sciences* **11**(5), 1633–1644.

Peters, W., van der Velde, I. R., Van Schaik, E., Miller, J. B., Ciais, P., Duarte, H. F., van der Laan-Luijkx, I. T., van der Molen, M. K., Scholze, M., Schaefer, K. et al. (2018), 'Increased water-use efficiency and reduced co 2 uptake by plants during droughts at a continental scale', *Nature geoscience* **11**(10), 744–748.

Piao, S., Ciais, P., Friedlingstein, P., Peylin, P., Reichstein, M., Luyssaert, S., Margolis, H., Fang, J., Barr, A., Chen, A. et al. (2008), 'Net carbon dioxide losses of northern ecosystems in response to autumn warming', *Nature* **451**(7174), 49–52.

Piao, S., Liu, Q., Chen, A., Janssens, I. A., Fu, Y., Dai, J., Liu, L., Lian, X., Shen, M. and Zhu, X. (2019), 'Plant phenology and global climate change: Current progresses and challenges', *Global change biology* **25**(6), 1922–1940.

Piao, S., Tan, J., Chen, A., Fu, Y. H., Ciais, P., Liu, Q., Janssens, I. A., Vicca, S., Zeng, Z., Jeong, S.-J. et al. (2015), 'Leaf onset in the northern hemisphere triggered by daytime temperature', *Nature communications* **6**(1), 1–8.

Piao, S., Wang, X., Park, T., Chen, C., Lian, X., He, Y., Bjerke, J. W., Chen, A., Ciais, P., Tømmervik, H. et al. (2020), 'Characteristics, drivers and feedbacks of global greening', *Nature Reviews Earth & Environment* **1**(1), 14–27.

Reichstein, M., Ciais, P., Papale, D., Valentini, R., Running, S., Viovy, N., Cramer, W., Granier, A., Ogee, J., Allard, V. et al. (2007), 'Reduction of ecosystem productivity and respiration during the european summer 2003 climate anomaly: a joint flux tower, remote sensing and modelling analysis', *Global Change Biology* **13**(3), 634–651.

Rigby, J. and Porporato, A. (2008), 'Spring frost risk in a changing climate', *Geophysical Research Letters* **35**(12).

Root, T. L., Price, J. T., Hall, K. R., Schneider, S. H., Rosenzweig, C. and Pounds, J. A. (2003), 'Fingerprints of global warming on wild animals and plants', *Nature* **421**(6918), 57–60.

Schwartz, M. D., Ahas, R. and Aasa, A. (2006), 'Onset of spring starting earlier across the northern hemisphere', *Global change biology* **12**(2), 343–351.

Smith, N. E., Kooijmans, L. M., Koren, G., van Schaik, E., van der Woude, A. M., Wanders, N., Ramonet, M., Xueref-Remy, I., Siebicke, L., Manca, G. et al. (2020), 'Spring enhancement and summer reduction in carbon uptake during the 2018 drought in northwestern europe', *Philosophical Transactions of the Royal Society B* **375**(1810), 20190509.

Sulla-Menashe, D. and Friedl, M. A. (2018), 'User guide to collection 6 modis land cover (mcd12q1) product', *NASA EOSDIS Land Processes DAAC: Sioux Falls, SD, USA* .

Sun, Y., Frankenberg, C., Jung, M., Joiner, J., Guanter, L., Köhler, P. and Magney, T. (2018), 'Overview of solar-induced chlorophyll fluorescence (sif) from the orbiting carbon observatory-2: Retrieval, cross-mission comparison, and global monitoring for gpp', *Remote Sensing of Environment* **209**, 808–823.

Sun, Y., Fu, R., Dickinson, R., Joiner, J., Frankenberg, C., Gu, L., Xia, Y. and Fernando, N. (2015), 'Drought onset mechanisms revealed by satellite solar-induced chlorophyll fluorescence: Insights from two contrasting extreme events', *Journal of Geophysical Research: Biogeosciences* **120**(11), 2427–2440.

Wang, S., Zhang, Y., Ju, W., Qiu, B. and Zhang, Z. (2021), 'Tracking the seasonal and inter-annual variations of global gross primary production during last four decades using satellite near-infrared reflectance data', *Science of the Total Environment* **755**, 142569.

Xia, J., Chen, J., Piao, S., Ciais, P., Luo, Y. and Wan, S. (2014), 'Terrestrial carbon cycle affected by non-uniform climate warming', *Nature Geoscience* **7**(3), 173–180.

Xu, L., Myneni, R., Chapin Iii, F., Callaghan, T. V., Pinzon, J., Tucker, C. J., Zhu, Z., Bi, J., Ciais, P., Tømmervik, H. et al. (2013), 'Temperature and vegetation seasonality diminishment over northern lands', *Nature climate change* **3**(6), 581–586.

Yu, H., Luedeling, E. and Xu, J. (2010), 'Winter and spring warming result in delayed spring phenology on the tibetan plateau', *Proceedings of the National Academy of Sciences* **107**(51), 22151–22156.

Yuan, W., Cai, W., Chen, Y., Liu, S., Dong, W., Zhang, H., Yu, G., Chen, Z., He, H., Guo, W. et al. (2016), 'Severe summer heatwave and drought strongly reduced carbon uptake in southern china', *Scientific Reports* **6**(1), 1–12.

Yuan, W., Zheng, Y., Piao, S., Ciais, P., Lombardozzi, D., Wang, Y., Ryu, Y., Chen, G., Dong, W., Hu, Z. et al. (2019), 'Increased atmospheric vapor pressure deficit reduces global vegetation growth', *Science advances* **5**(8), eaax1396.

Zhang, Y., Song, C., Band, L. E., Sun, G. and Li, J. (2017), 'Reanalysis of global terrestrial vegetation trends from modis products: Browning or greening?', *Remote Sensing of Environment* **191**, 145–155.

Zhu, Z., Piao, S., Myneni, R. B., Huang, M., Zeng, Z., Canadell, J. G., Ciais, P., Sitch, S., Friedlingstein, P., Arneth, A. et al. (2016), 'Greening of the earth and its drivers', *Nature climate change* **6**(8), 791–795.

Zohner, C. M. and Renner, S. S. (2015), 'Perception of photoperiod in individual buds of mature trees regulates leaf-out', *New Phytologist* **208**(4), 1023–1030.